OPEN

Molecular Psychiatry (2018) 23, 521–532

www.nature.com/mp

ORIGINAL ARTICLE

Evidence for newly generated interneurons in the basolateral amygdala of adult mice

DJ Jhaveri[1,2,5], A Tedoldi[1,5], S Hunt[1], R Sullivan[1], NR Watts[3], JM Power[4], PF Bartlett[1,6] and P Sah[1,6]

New neurons are continually generated from the resident populations of precursor cells in selective niches of the adult mammalian brain such as the hippocampal dentate gyrus and the olfactory bulb. However, whether such cells are present in the adult amygdala, and their neurogenic capacity, is not known. Using the neurosphere assay, we demonstrate that a small number of precursor cells, the majority of which express Achaete-scute complex homolog 1 (Ascl1), are present in the basolateral amygdala (BLA) of the adult mouse. Using neuron-specific Thy1-YFP transgenic mice, we show that YFP+ cells in BLA-derived neurospheres have a neuronal morphology, co-express the neuronal marker βIII-tubulin, and generate action potentials, confirming their neuronal phenotype. *In vivo*, we demonstrate the presence of newly generated BrdU-labeled cells in the adult BLA, and show that a proportion of these cells co-express the immature neuronal marker doublecortin (DCX). Furthermore, we reveal that a significant proportion of GFP+ neurons (~23%) in the BLA are newly generated (BrdU+) in DCX-GFP mice, and using whole-cell recordings in acute slices we demonstrate that the GFP+ cells display electrophysiological properties that are characteristic of interneurons. Using retrovirus-GFP labeling as well as the Ascl1^{CreERT2} mouse line, we further confirm that the precursor cells within the BLA give rise to mature and functional interneurons that persist in the BLA for at least 8 weeks after their birth. Contextual fear conditioning has no effect on the number of neurospheres or BrdU-labeled cells in the BLA, but produces an increase in hippocampal cell proliferation. These results demonstrate that neurogenic precursor cells are present in the adult BLA, and generate functional interneurons, but also show that their activity is not regulated by an amygdala-dependent learning paradigm.

Molecular Psychiatry (2018) **23,** 521–532; doi:10.1038/mp.2017.134; published online 15 August 2017

INTRODUCTION

Overwhelming evidence has established that the addition of new neurons continues in discrete areas of the adult mammalian brain, particularly in the olfactory bulb and the dentate gyrus of the hippocampus.[1] The resident populations of neural stem and precursor cells, which proliferate and differentiate into functional neurons, drive neurogenesis in these regions.[2–4] Numerous studies have shown that this form of cellular plasticity plays a critical role in regulating functions associated with these regions, such as olfactory discrimination, spatial learning and emotion.[2,5–10]

Although the occurrence of neurogenesis has been proposed for other 'non-canonical' neurogenic regions of the adult brain,[11–13] the characteristics of any resident neural precursor cells, the factors that regulate their differentiation potential, maturation and integration into the local circuitry, and their functional contribution remain unclear.[14–16] Given the pivotal role of the amygdala in the acquisition, consolidation and expression of emotional memories,[17,18] there has been considerable interest in determining the presence and possible functional role of neurogenesis in this region. Moreover, the amygdala is thought to be a key player in a host of anxiety-related disorders including generalized anxiety and post-traumatic stress,[19] and monoamine reuptake blockers are widely used for the treatment of many of these disorders. Although the cellular mechanisms underlying their therapeutic actions are not completely clear, it has been suggested that these compounds alter neurogenesis in the adult brain.[20] Thus, it is of interest to understand whether, and what subtypes of new neurons are generated in the amygdala, which may provide insight into how this form of cellular plasticity alters the existing microcircuitry and ultimately exerts an effect on behavior.

Although one report in monkeys[21] has suggested the presence of newly generated neurons in the adult amygdala, whether these newborn neurons are functional remains unclear. In fact, several studies using rodents have reported that newly generated cells could only be detected in this brain region following stimulation,[22–24] and notably they only generated non-neuronal populations.[23–25] However, the origin of these new cells, and whether the amygdala, similar to the adult hippocampus and subventricular zone (SVZ), contains a resident population of precursor cells capable of generating functional neurons[3,4,26] are not known. Recent findings have highlighted the presence of large populations of quiescent precursor cells in the hippocampus that are activated by distinct neurogenic stimuli such as neuronal depolarization and the neurotransmitter norepinephrine.[4,27,28] We therefore asked whether the adult amygdala also harbors such quiescent precursor cell populations. As growing evidence

[1]The University of Queensland, Queensland Brain Institute, Brisbane, QLD, Australia; [2]Mater Research Institute, The University of Queensland, Brisbane, QLD, Australia; [3]Critical Care and Trauma Division, The George Institute for Global Health, Sydney, NSW, Australia and [4]School of Medical Science, University of New South Wales, Sydney, NSW, Australia. Correspondence: Dr DJ Jhaveri or Professor PF Bartlett or Professor P Sah, The Queensland Brain Institute, University of Queensland, Hawken Drive, St Lucia, 4072 QLD, Australia. E-mail: dhanisha@uq.edu.au or p.bartlett@uq.edu.au or pankaj.sah@uq.edu.au

[5]These authors contributed equally to this work.

[6]These authors contributed equally to this work.

Received 15 February 2015; revised 2 May 2017; accepted 8 May 2017; published online 15 August 2017

indicates that neural stem cells are heterogeneous and exhibit differences in their proliferative, self-renewal and differentiation capacities, we have used 'precursor' as a generic term to include cells that have both stem- and progenitor-like properties.

In this study we tested for the presence of both active and quiescent precursor cell populations within the adult amygdala, and investigated their neurogenic potential. We characterized the electrophysiological properties of newly generated neurons, and, given the central role of the amygdala in fear learning,[29,30] examined whether such learning regulates the activity of these cells.

MATERIALS AND METHODS

Animals

Adult (7–12-week old) male C57BL/6J mice expressing yellow fluorescent protein (YFP) under the control of the thymocyte antigen 1 (Thy1) promoter,[31] mice expressing enhanced green fluorescent protein (GFP) under the control of the doublecortin (DCX) promoter,[32] mice expressing GFP under the control of the chicken beta-actin promoter in all cells (AGFP mice),[33] mice expressing GFP under the control of glutamic acid decarboxylase (GAD67) promoter[34] and tamoxifen-inducible mice expressing the tdTomato reporter under the control of Achaete-scute complex homolog 1 (Ascl1)-Cre^{ERT2} (Ascl1^{CreERT2}; CAG$^{floxStop\text{-}tdTomato}$ mice obtained from Jackson Laboratory, Bar Harbor, ME, USA, stock #012882)[35] were used for the experiments conducted in this study. To label proliferating cells *in vivo*, DCX-GFP mice were administered 5-bromo-2-deoxyuridine (BrdU; 100 mg kg^{-1}; Sigma-Aldrich Castle Hill, NSW, Australia) intraperitoneally twice daily for 14 days and were killed either 24 h or 4 weeks later. Seven to 8-week-old male Ascl1^{CreERT2}; CAG$^{floxStop\text{-}tdTomato}$ mice were administered tamoxifen intraperitoneally at 180 mg kg^{-1} for three consecutive days. Animals were killed 4 or 8 weeks after the last tamoxifen injection and brain tissue was harvested for electrophysiological recordings and immunohistochemistry.

All mice were housed in groups (3–5 mice per cage) and maintained on a 12 h light/dark cycle with *ad libitum* access to food and water. Treatments and procedures were carried out in accordance with the Australian Code of Practice for the Care and Use of Animals for Scientific Purposes and were approved by the University of Queensland Animal Ethics Committee.

Amygdala dissection and neurosphere assay

Mice were killed by cervical dislocation and their brains removed in cold artificial cerebrospinal fluid (aCSF) containing 118 mM NaCl, 2.5 mM KCl, 25 mM $NaHCO_3$, 10 mM D-glucose, 1.2 mM NaH_2PO_4, 1.3 mM $MgCl_2$ and 2.5 mM $CaCl_2$. Coronal brain slices (500 μm) were then prepared on a vibratome (Leica, Mt Waverley, VIC, Australia). The basolateral amygdala (BLA) and hippocampus were microdissected from these slices under a binocular microscope to ensure that there was no contamination from the surrounding tissue. The tissues were then individually minced using scalpel blades, and neural precursor activity was examined using the neurosphere assay as described previously.[27] Briefly, the minced tissue was digested using 0.1% papain or 0.1% trypsin-EDTA (Invitrogen, Zug, Switzerland) to obtain a single-cell suspension. The cell suspension was centrifuged at 700 r.p.m. for 5 min and the pellet was washed before being plated in a 24- or 96-well plate and cultured in complete neurosphere medium containing epidermal growth factor (EG;F; 20 ng ml^{-1}) and basic fibroblast growth factor (bFGF; 10 ng ml^{-1}), in the presence or absence of L-(−)-noradrenaline (+)-bitartrate salt monohydrate (norepinephrine; 10 μM) or potassium chloride (KCl, 15 mM). The number and the size of primary neurospheres obtained were determined on day 10.

Neurosphere differentiation

Primary neurospheres derived from the BLA were collected and plated onto coverslips coated with poly-D-lysine in 24-well plates and differentiated in a serum-free medium containing DMEM/F12 with proliferation supplements (Stem Cell Technologies, Tullamarine, VIC, Australia). On day 5, the neurospheres were fixed using ice-cold 4% paraformaldehyde and washed several times with phosphate-buffered saline (PBS). Following blocking with 3% normal goat serum, they were then incubated in a solution containing primary antibodies at 4 °C overnight. The primary antibodies used were mouse anti-ßIII tubulin (1:2000, Promega, Sydney, NSW, Australia), rabbit anti-GFAP (1:500, Dako), rat anti-myelin basic protein (MBP; 1:500; Millipore, Schaffausen, Switzerland), rabbit anti-glial fibrillary acidic protein (GFAP;1:5000, DakoCytomation, Oyster Point Blvd, South San Francisco, CA, USA), mouse anti-GAD-67 (Chemicon, Boronia, VIC, Australia: 1:10000) and anti-pan sodium channel (Alomone, Jerusalem, Israel: 1:500). Following PBS washes, Alexa Fluor 568 anti-mouse (1:1000, Invitrogen), Alexa Fluor 488 or 568 anti-rabbit (1:1000, Invitrogen) or Alexa Fluor 488 anti-rat (1:1000, Invitrogen) secondary antibodies were applied together with DAPI (1:1000, Sigma-Aldrich). Finally, coverslips were applied using fluorescence mounting medium (Dako, Mulgrave, VIC, Australia). Secondary antibody-only controls were also run to control for non-specific labeling.

Stereotaxic surgery for retrovirus-GFP delivery

Eight-week-old male C57BL/6J mice were anesthetized with ketamine/xylazine (100/20 mg kg^{-1}, i.p.), and fixed in a stereotaxic frame. The skull was then exposed and a hole was drilled over each BLA, which was identified based on stereotaxic coordinates from Bregma (mm): − 1.5 anteroposterior, ± 3 mediolateral, − 3.4 dorsoventral (Figure 5a). Retrovirus (2 μl) was infused into this region bilaterally using a glass-pipette attached to a 2 μl Hamilton syringe. The murine Moloney leukemia virus-based retroviral vector expressing GFP (Clontech, Clayton, VIC, Australia) was prepared as described in detail previously,[36] at a titer of ~ 10^6 c.f.u. per ml. Once the infusion was complete, the skull was closed and the skin sutured using Vetbond. Animals were administered the analgesic Metacam (2 mg kg^{-1}) Boehringer Ingelheim, NSW, Australia and the antibiotic Baytril (5 mg kg^{-1}, Bayer, Gordon, NSW, Australia) to facilitate recovery. Animals were used for electrophysiological recordings 7–8 weeks after retrovirus injections.

Electrophysiology

For electrophysiological recordings, neurospheres were prepared from Thy1-YFP animals as detailed above. After 10 days in culture, cells expressing YFP were identified under a fluorescence microscope (Zeiss 710, Clayton, VIC, Australia). Whole-cell recordings were obtained from YFP-positive (YFP+) cells using a K-methyl-sulfate based internal solution containing 135 mM $KMeSO_4$, 5 mM NaCl, 10 mM Hepes, 2 mM Mg_2-ATP, 0.3 mM Na_3-GTP, 0.3 mM EGTA, 0.1 mM spermine and 7 mM phosphocreatine (pH = 7.3, ~ 290 mOsmol). Data were collected using Axograph X software and a Multiclamp 700B amplifier (Molecular Devices). Signals were filtered at 10 kHz and digitized at 50 kHz using an ITC-16A/D converter (InstruTech, Longmont, CO, USA).

Whole-cell recordings were obtained from DCX-GFP-positive (DCX-GFP+) cells in acute brain slices from DCX-GFP mice, GFP-positive (GFP+) cells from retrovirus-injected mice and tdTomato-positive (tdTom+) cells from Ascl1^{CreERT2}; CAG$^{floxStop\text{-}tdTomato}$ mice. Mice were anesthetized with isoflurane, decapitated, and 300 μm thick coronal brain slices prepared in an ice-cold sucrose solution (87 mM NaCl, 25 mM $NaHCO_3$, 25 mM glucose, 50 mM sucrose, 2.5 mM KCl, 1.2 mM NaH_2PO_4, 4 mM $MgCl_2$, 0.5 mM $CaCl_2$), using a vibratome (Leica). The slices were allowed to recover in oxygenated aCSF for 30 min at 32 °C and then at room temperature until required. Brain slices were continuously perfused with oxygenated aCSF (32 °C) and whole-cell patch-clamp recordings were performed using a Multiclamp 700B (Molecular Devices), and analyzed using AxoGraph (AxoGraphX). Glass recording electrodes (4–7 MΩ, Harvard Apparatus glass capillaries, Narishige PC-10 electrode puller) were filled with a K-methyl-sulfate internal solution containing 135 mM KMeSO4, 8 mM NaCl, 10 mM HEPES, 2 mM MgATP, 0.3 mM GTP, 7 mM phosphocreatine, 0.2 mM EGTA and 0.2% biocytin (pH 7.2 with KOH, 295 mOsmol). For DCX-GFP+ cell recordings, spiking was evoked using current injections applied in increments of 20 pA from − 60 to 120 pA. In the case of paired recordings, an action potential was evoked by a short current injection (5 ms, 600 pA) delivered to the first cell in current clamp, while the second cell was monitored for a response in voltage and current clamp. For GFP+ and tdTom+ cell recordings, spikes were evoked by injecting current from − 60 to 120 pA (20 pA increments) and from − 10 to 340 pA (50 pA increments) to record spontaneous potential events and spiking, respectively. In the case of spontaneous excitatory postsynaptic current (sEPSC) recordings, GFP+and tdTom+ cells were voltage-clamped at − 60 mV and recorded for 10 min. Input resistance, action potential threshold, amplitude, delay, half-width, rise time and sEPSCs were analyzed offline.

Fear conditioning

Contextual fear conditioning was performed using a VideoFreeze system from Med Associates. Conditioned animals received a single training

session daily for six consecutive days. For each session mice were placed in a distinctive context (the shock chamber) and after an initial baseline period of 2 min, received 5 footshocks (0.8 mA, 1 s) through the grid floor over a 20 min period. BrdU (100 mg kg^{-1}) was administered via intraperitoneal injections, given twice daily, 6 h apart following training, and mice were killed 24 h after the final injection. Immediately prior to killing, contextual fear conditioning was assayed by measuring freezing upon re-exposure to the conditioning context for 4 min in the absence of footshock. Freezing was quantified using automatic freezing detection software (Med Associates), and expressed as a percentage of time spent freezing across the test session. Naive animals served as controls, receiving injections in the animal housing facility. Animals used for the neurosphere assay experiment did not receive any BrdU injections.

Immunohistochemistry

Mice were injected with an overdose of sodium pentobarbitone (100 mg kg^{-1}) and were transcardially perfused with 1% sodium nitrate in 0.1M phosphate buffer (PB, pH 7.2) followed by 4% paraformaldehyde in 0.1M PB (pH 7.2). Brains were removed from the skull and post-fixed via immersion in the same fixative for 3 h at room temperature on an orbital shaker. Brains were washed in 0.1M PBS and stored at 4 °C with 0.05% sodium azide until sectioned. Coronal sections, 50 µm thick, were cut using a vibratome (Lecia 1000 s) along the entire rostro-caudal axis containing the amygdala and the hippocampus. Every fourth section was used for immunohistochemical analysis. For BrdU immunolabeling, the sections were briefly rinsed in 0.1M PBS, then incubated in 1M HCl at 45 °C for 20 min. Sections were rinsed in boric acid (pH 6) for 5 min, followed by a wash in 0.1M PBS, and were then placed into a 3% bovine serum albumin (BSA, Sigma-Aldrich) solution for 1 h. Following this, the sections were incubated in a 1% BSA solution containing the primary antibodies, including rat anti-BrdU (1:1000, Accurate Chemical, Westbury, NY, USA), rabbit anti-DCX (1:2000, Abcam) or guinea pig anti-DCX (1:500, Millipore), rabbit anti-GFAP (1:5000, DakoCytomation, Glostrup, Denmark), chicken anti-GFP, (1:4000, Aves Labs, Tigard, OR, USA), rabbit anti-Ki67 (1:500, Novacastra, Mt Waverley, VIC, Australia), rabbit anti-Iba1 (1:1000, Wako, Richmond, VA, USA), mouse anti-NeuN (1:1000, Millipore), rat anti-tdTomato (1:2500, Kerafast, Boston, MA, USA), mouse anti-calbindin (1:1000, Sigma), and rabbit calretinin (1:1000, Swant, Marley, Switzerland). Following incubation with the primary antibodies, sections were washed in PBS and incubated in the appropriate species-specific secondary antibody in a 1% BSA solution for 5 h (1:1000, Invitrogen). To visualize cells filled with biocytin, brain slices were incubated with streptavidin (1:2000) in a 1% BSA solution overnight. Sections were incubated in DAPI (1:1000) to stain the nuclei of cells, and then mounted on microscope slides with fluorescence mounting medium.

Quantification

Fluorescence immunolabeling was visualized and imaged on a confocal laser-scanning microscope (LSM 710, Zeiss, Clayton, VIC, Australia) or a spinning-disk confocal system (Marianas; Intelligent Imaging Innovations, Denver, CO, USA) consisting of an Axio Observer Z1 (Carl Zeiss, North Ryde, NSW, Australia) equipped with a CSU-W1 spinning-disk head (Yokogawa Corporation of America), ORCA-Flash4.0 v2 sCMOS camera (Hamamatsu Photonics, Shizuoka, Japan), and ×40 1.2 NA C-Apo objectives. Image acquisition was performed using SlideBook 6.0 (Intelligent Imaging Innovations). The resulting images were processed and visualized using Imaris 7.7 software (Bitplane, Concorde, MA, USA). Cell counts were performed on image stacks using Imaris or Fiji. Labeled cells were quantified along the rostral-caudal extent of the amygdala by carefully determining the boundaries of each nucleus using a standard neuroanatomical atlas. BrdU-labeled cells were represented as cells per mm^2 of the BLA and co-labeled cells were represented as the percentage of total BrdU-positive (BrdU+) cells. In the hippocampus, BrdU-labeled cells were quantified from the granule cell layer and represented as cells per mm length of the dentate gyrus.

Statistical analysis

All data are expressed as mean ± s.e.m. Statistical analyses were performed using GraphPad Prism (GraphPad Software, La Jolla, CA, USA). A Student's unpaired *t*-test was used for experiments with two groups and a one-way analysis of variance with a Bonferroni *post hoc* test was used for experiments involving more than two groups. Significance was determined at $P < 0.05$. A *post hoc* power analysis was conducted to ascertain that the electrphysiology data were obtained from sufficient number of cells. For example, power analysis for the difference in the input resistance observed between the principal neurons ($n = 5$) and 4-week-old tdTom+ neurons ($n = 5$) revealed that in order for an effect of this size (mean difference = 118) to be detected (80% chance) as significant at the 5% level (Figure 5h), a sample of five cells is sufficient. Power analysis for the difference in the action potential half-width (Figure 5i) between the principal neurons ($n = 5$) and 7–8-week-old GFP+ neurons ($n = 6$) revealed that in order for an effect of this size (mean difference = 0.26) to be detected (80% chance) as significant at the 5% level (Figure 5h), a sample of 4 cells is sufficient.

RESULTS

The BLA harbors a resident population of precursor cells

To test for the presence of an endogenous pool of precursor cells within the amygdala, we used the neurosphere assay[37] to isolate and characterize this population. The BLA was microdissected from acutely prepared C57BL/6 brain slices (Figure 1a), dissociated, and a single-cell suspension was plated in control neurosphere medium containing EGF and bFGF at a low cell density of < 5 cells per µl. Following 10 days in culture, neurospheres could be seen (Figure 1b). On average, 11.5 ± 1.9 BLA-derived neurospheres were obtained per brain (Figure 1c; $n = 9$), suggesting the presence of a small population of precursor cells. We have previously shown that the addition of KCl to depolarize cells,[4] or stimulation of β-adrenergic receptors with norepinephrine[27] can activate latent neurogenic precursors in the hippocampus. We therefore tested if similar treatments would also activate latent precursor cells and increase the number of neurospheres generated from the adult amygdala. Neither KCl (15 mM) nor norepinephrine (10 µM) altered the total number of neurospheres obtained (KCl: 11.8 ± 2.1 neurospheres; norepinephrine: 15.4 ± 2.6 neurospheres, $n = 9$, $P > 0.05$) as compared to control conditions (Figure 1c). However, both treatments led to a significant increase in the size of the neurospheres, particularly those measuring > 200 µm in diameter (Figure 1d). The clonal origin of the BLA-derived neurospheres was confirmed using mixtures of differently labeled precursor cells from wild-type and AGFP mice (Supplementary Figure S1).

To determine the identity of neurosphere-forming precursors residing within the BLA, we used a genetically modified mouse that expresses inducible Cre recombinase under the Ascl1promoter. Recent studies have shown that Ascl1, a bHLH transcription factor, is expressed by a subset of neural precursor cells residing in the adult hippocampus and SVZ, and Ascl1^{CreERT2} mice can been used to study the development and functional integration of newborn neurons in these neurogenic niches.[35,38,39] To investigate whether neural precursors in the BLA also express Ascl1, we crossed Ascl1^{CreERT2} mice to the CAG$^{floxStop\text{-}tdTomato}$ (Ai14) conditional reporter line to achieve indelible expression of tdTomato in neural precursors and their progeny. Seven- to 8-week-old Ascl1^{CreERT2}; CAG$^{floxStop\text{-}tdTomato}$ mice were administered tamoxifen and the BLA was microdissected for the neurosphere assay. Consistent with our data from the C57BL/6 mice, neurospheres were obtained in the control condition as well as in the presence of norepinephrine or KCl. Notably, the majority ($> 70\%$) of these BLA-derived neurospheres were tdTom+ (Figure 1e and f) demonstrating that precursors in the BLA express the proneural gene Ascl1.

Together, these results suggest that precursor cells, the majority of which are Ascl1+, are present in the BLA but unlike in the adult hippocampus, this region does not contain latent precursor cells that can be activated *in vitro*. Rather, in the amygdala, both depolarizing stimuli (KCl) and norepinephrine enhance the proliferation of already active precursor cells.

Neural precursor cells in the amygdala have neurogenic capacity and generate functional neurons *in vitro*

To determine whether the precursor cell population isolated from the amygdala was neurogenic, we differentiated neurospheres

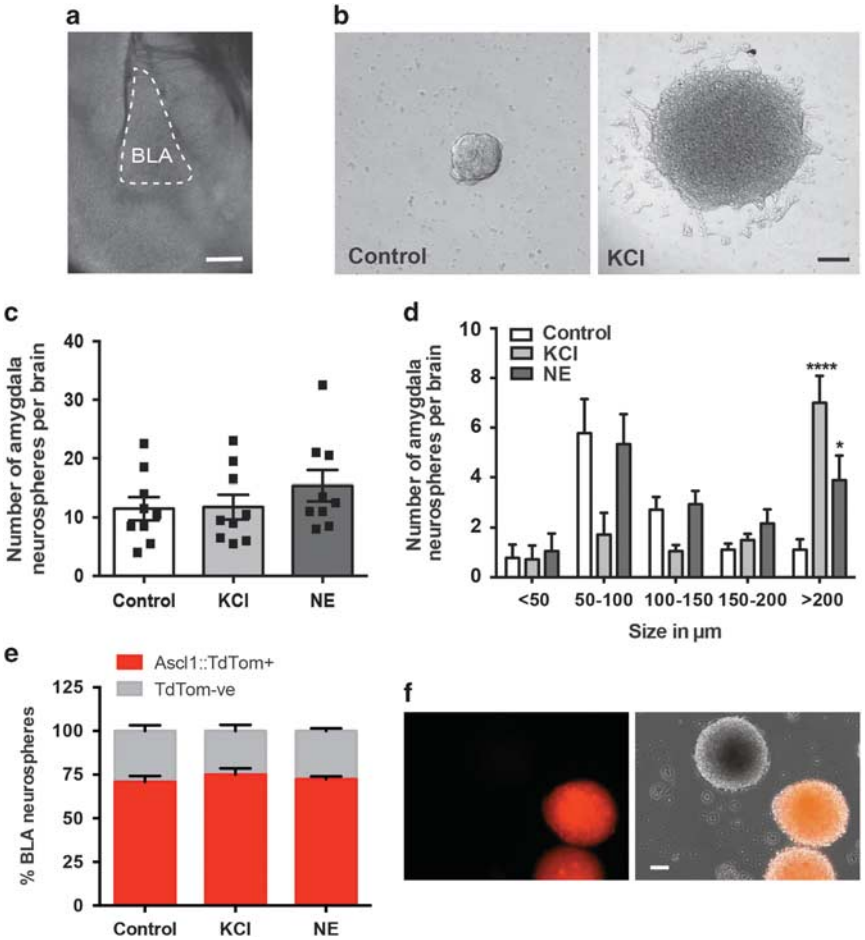

Figure 1. Presence of precursor cells in the basolateral amygdala (BLA). (**a**) The BLA was microdissected from 500 μm thick coronal brain slices. (**b**) Photomicrograph of a neurosphere obtained in control medium versus medium containing 15 mM KCl. (**c**) Similar numbers of BLA-derived neurospheres per brain were obtained in control, norepinephrine- (10 μM, NE) and KCl-treated wells ($n = 9$). (**d**) Distribution of neurospheres based on their size in control, NE and KCl conditions. Note the significant increase in the number of neurospheres measuring >200 μm in the NE and KCl treatment conditions compared with the control ($n = 9$, $^*P < 0.05$, $^{****}P < 0.0001$). (**e**) The majority of neurospheres generated from the BLA are derived from Ascl1-expressing precursor cells (Ascl1::tdTom+) labeled using $Ascl1^{CreERT2}$; $CAG^{floxStop\text{-}tdTomato}$ mice. (**f**) Examples of BLA-derived Ascl1::tdTom+ and tdTom− neurospheres. Scale bars, 100 μm.

derived from the amygdala of Thy1-YFP mice. The regulatory elements of the *thy1.2* gene used to generate this strain of mice have been shown to drive neuron-specific expression of the fluorescent protein YFP in the adult brain.[31] To increase precursor cell proliferation, cells isolated from the BLA of Thy1-YFP mice were treated with KCl or norepinephrine. Upon differentiation, YFP + cells were observed in these neurospheres (Figure 2a and b), and 52% of the cells co-expressed the immature neuronal marker βIII tubulin ($n = 92$ YFP+ cells) (Figure 2b). To confirm that the YFP+ cells generated within the amygdala-derived neurospheres were neurons, we investigated their electrophysiological properties (Figure 2d and e). Whole-cell recordings from YFP+ cells showed that these cells had a resting membrane potential of -55 ± 11 mV, an input resistance of 293 ± 331 MΩ, and a membrane time constant of 4.7 ± 3.3 ms ($n = 5$). Depolarizing current injections evoked small amplitude action potentials (Figure 2e), similar to those seen in early newborn neurons in the dentate gyrus,[32] thereby confirming their neuronal phenotype. Interestingly, a small proportion of neurospheres (3/10) also contained a few GAD67+ cells (Figure 2c), suggesting that a proportion of amygdala-derived precursor cells have the capacity to differentiate into GABAergic neurons. The interneuron-generating capacity of the precursor cells in the BLA was further confirmed using neurospheres derived from GAD67-GFP mice which showed that the majority (95 out of 128 neurosphres) of BLA-generated neurospheres contained GFP+ cells.

We also examined whether the neurosphere-forming precursors in the BLA were multipotent *in vitro*. All of the BLA-derived neurospheres examined ($n = 70$ neurospheres) contained both βIII tubulin+ neurons, and GFAP+ astrocytes. 65% ($n = 20$ neurospheres) also contained MBP+ oligodendrocytes (Supplementary Figure S2). Collectively, these results demonstrate that the adult amygdala harbors populations of bipotent as well as multipotent precursor cells.

Proliferating cells within the amygdala are neurogenic *in vivo*

Having shown that the adult BLA contains a precursor cell population that can generate neurons *in vitro,* we next examined whether and what proportion of the proliferating cells within the adult amygdala differentiate into neurons *in vivo*, by injecting mice intraperitoneally with BrdU. Following 14 days of injection, BrdU+ cells were seen in the BLA (Figure 3a) at a density of 62.1 ± 4.7 cells per mm^2 ($n = 4$ mice). Ki67, an endogenous marker of cell proliferation, also labeled cells within the BLA (51.9 ± 7.1 cells per mm^2; $n = 3$ mice; Supplementary Figure S3),

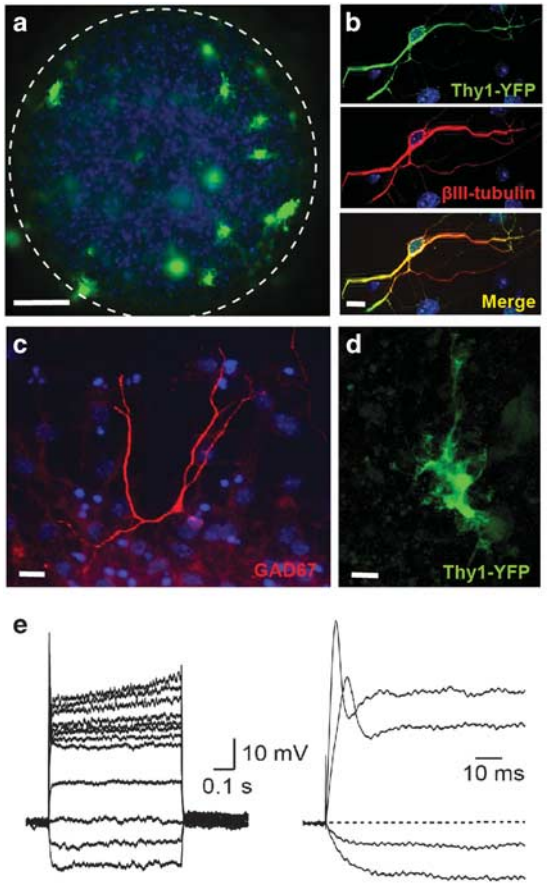

Figure 2. BLA-derived neurospheres contain functional neurons. (**a**) Several Thy1- YFP+ cells are present in a basolateral amygdala (BLA)-derived neurosphere. Nuclei are stained with DAPI (blue) Scale bar, 50 μm. (**b**) Higher magnification of a fixed Thy1-YFP+ neuron (green) co-labeled with βIII-tubulin (red). Scale bar, 10 μm (**c**) An example of a GAD67+ neuron in a BLA-derived neurosphere. (**d**, **e**) Whole-cell recordings from YFP+ cells (scale bar, 10 μm), showing that depolarizing current injections evoke small amplitude action potentials (**e**).

thereby confirming that proliferating cells are present in this region. To determine whether these BrdU+ cells differentiate into neurons, we first quantified the number of BrdU+ cells expressing the immature neuronal marker DCX, and found that 8.2 ± 1.8% of BrdU-labeled cells co-expressed DCX in the BLA (Figure 3b; $n = 4$ mice). This was further confirmed using DCX-GFP mice, in which GFP+ neurons in the adult dentate gyrus have the properties of newly born neurons.[32] In the BLA, 23.2 ± 1.9% of GFP+ ($n = 4$ mice) cells were co-labeled for BrdU, consistent with them being adult-born cells (Figure 3c). To test whether proliferating cells in the BLA also adopt a glial fate, BrdU+ cells were co-labeled for the glial markers GFAP (for astrocytes) or Iba1 (for microglia). We found that 23.3 ± 7.8% of BrdU+ cells expressed GFAP whereas 27.5 ± 6.3% expressed Iba1 ($n = 3$ mice; Supplementary Figure S3), demonstrating that a proportion of the newly generated cells in the BLA have a glial fate.

We next determined the long-term fate of the newly generated cells in the DCX-GFP mice by quantifying the proportion of BrdU+ cells that expressed the mature neuronal marker NeuN at 4 weeks after the last BrdU injection. We found that 8.4 ± 0.7% of the BrdU+ cells co-labeled for NeuN, but had no GFP expression (Figure 3d, $n = 3$ mice), demonstrating that a small proportion of newly generated cells in the BLA become mature neurons. Interestingly, 13.9 ± 3.1% of BrdU+ cells retained expression of DCX-GFP while expressing NeuN (Figure 3e, $n = 3$ mice), suggesting that these cells may represent an intermediate population.

DCX-expressing cells in the BLA exhibit the electrophysiological properties of interneurons

Having demonstrated the presence of newly generated DCX-GFP+ cells in the BLA, we next investigated their electrophysiological properties. Whole-cell recordings from DCX-GFP+ cells in the BLA (Figure 4a; $n = 42$ cells) revealed that these cells had a resting membrane potential of − 56 ± 8 mV. Of the 42 cells recorded, 23 were successfully recovered for anatomical analysis, and displayed a range of morphologies from mature cells with branching dendrites (Figure 4c) to 'underdeveloped' and sparsely branching cells (Figure 4f). Consistent with this morphological variety, DCX-GFP+ cells showed a broad distribution of input resistance (Figure 4b). Moreover, cells with developed dendritic trees had lower input resistances, displayed a high frequency of spontaneous synaptic events, and discharged with high frequency action potentials in response to depolarizing current injection (Figure 4c–e). In contrast, cells with short dendrites had a higher input resistance, showed little spontaneous synaptic activity and typically only discharged a few action potentials (Figure 4f–h). Overall, cells with an input resistance less than 400 MΩ had action potentials with a half-width of 0.92 ± 0.08 ms ($n = 13$), whereas the action potentials in cells with high input resistance ($>$ 600 MΩ) had a significantly wider half-width of 1.17 ± 0.06 ms ($n = 16$; $P < 0.02$). For comparison, mature pyramidal neurons had action potentials with a half-width of 1.3 ± 0.1 ms ($n = 6$). Together, these electrophysiological properties of DCX-GFP+ cells are similar to those of interneurons in the BLA;[40,41] the different input resistance and distribution of action potential duration suggest that the cells which are present in the BLA are at different developmental stages.

To confirm that these neurons were indeed interneurons, paired whole-cell recordings were made between DCX-GFP+ neurons and principal neurons (Figure 4j). In these recordings, a single action potential was evoked in the presynaptic DCX-GFP+ cell while the postsynaptic neuron was voltage clamped at − 40 mV. One out of six dual recordings between a DCX-GFP+ neuron and a principal neuron showed that an action potential in a DCX-GFP+ neuron evoked an outward current that was significantly smaller near the chloride reversal potential (Figure 4i). In current clamp, an action potential in the presynaptic neuron evoked a hyperpolarization (Figure 4k), showing that DCX-GFP+ neurons make inhibitory synapses with principal neurons.

Retroviral birth-dating and lineage tracing using Ascl1^{CreERT2} mice show that newborn neurons exhibit the electrophysiological properties of interneurons in the BLA

Two approaches were used to confirm that functional newborn neurons are indeed generated in the BLA. In the first of these, we used a retrovirus-expressing GFP that labels dividing cells and has been widely used to study functional neurogenesis in the adult hippocampus.[42–44] In the second approach, we used Ascl1^{CreERT2} mice to label newborn neurons in the BLA and characterize their functional properties. Retrovirus expressing GFP was injected into the BLA and electrophysiological recordings from GFP+ cells were performed 7–8 weeks later (Figure 5a–c and Supplementary Figure 4). Whole-cell patch-clamp recordings from GFP+ cells ($n = 6$ cells) revealed that these cells discharged action potentials and received synaptic input, as seen by the presence of spontaneous excitatory synaptic potentials and sEPSCs (Figure 5c and Supplementary Figure S4c). More importantly, these cells exibited passive and active membrane properties that were different from those of principal neurons within the BLA (Figure 5i

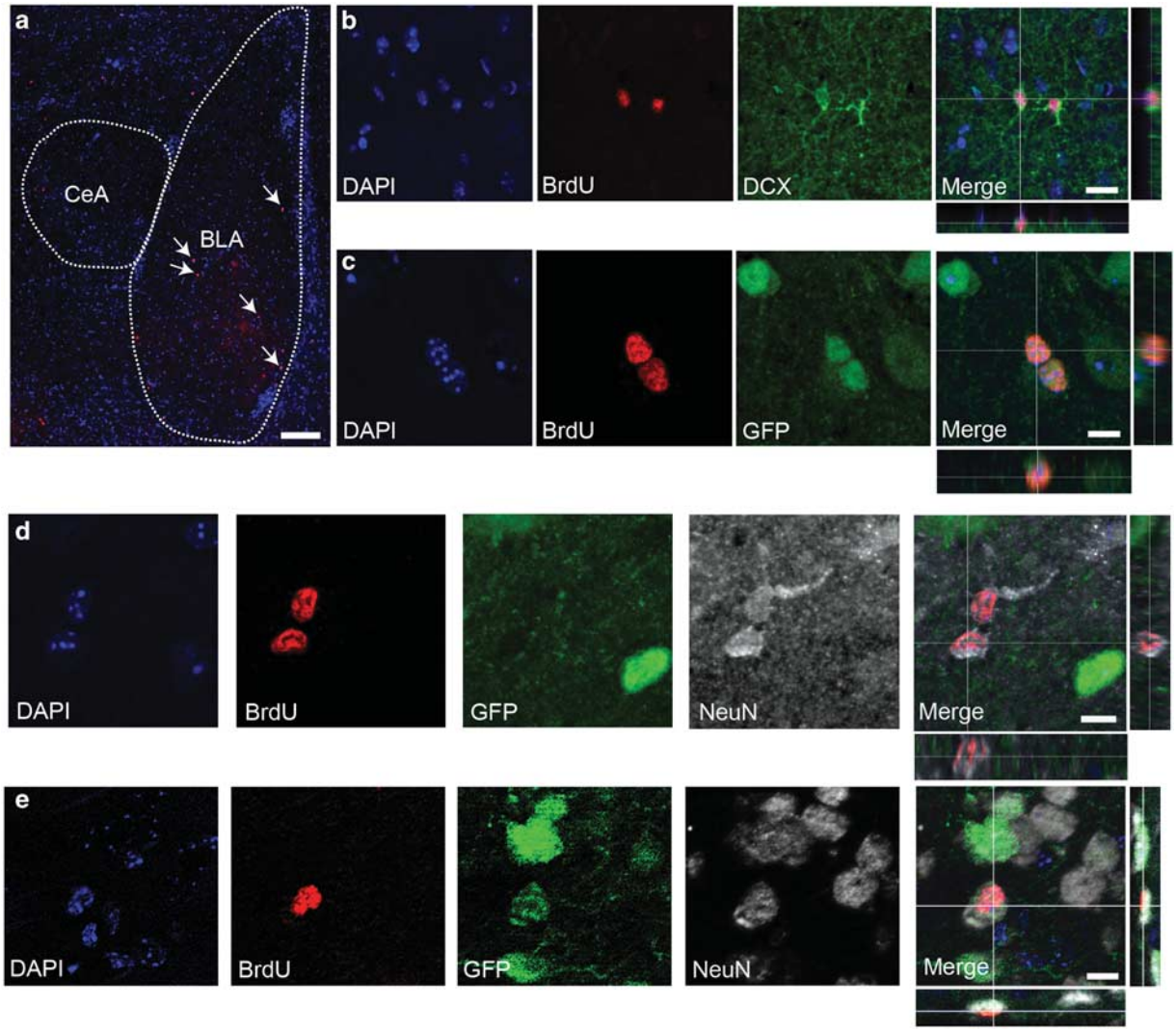

Figure 3. New neurons are generated in the amygdala nuclei *in vivo*. (**a**) BrdU-labeled cells (red, arrows) are present in the basolateral amygdala (BLA) in adult mice. CeA: central amygdala (**b**) An example of BrdU-labeled cells (red) co-expressing the immature neuronal marker DCX (green) in the BLA. All nuclei are labeled with DAPI (blue). (**c**) An example of DCX-GFP+ cells (green) in the BLA that are co-labeled with BrdU (red). The merged image and orthogonal views are shown on the far right. (**d**) DCX-GFP−, BrdU+ cells co-labeled with the mature neuronal marker NeuN in the BLA 4 weeks after the last BrdU injection. (**e**) A BrdU-labeled cell co-expressing DCX-GFP and NeuN. Scale bars, 50 μm in (**a**) and 10 μm in (**b**–**e**).

and Supplementary Figure S4g–j). The resting membrane potential of GFP+ neurons was −62.6 ± 0.8 mV, significantly more depolarized than that of principal neurons (−69.6 ± 1.4 mV, $P < 0.05$). Moreover, current-clamp recordings of trains of action potentials showed that the GFP+ cells had faster action potentials than principal neurons (action potential half-width of 1.0 ± 0.03 ms versus 1.3 ± 0.1 ms, $P < 0.05$), as well as a lower action potential threshold (−40.3 ± 1.3 mV versus -29.9 ± 1.3 mV, $P < 0.01$), lower action potential rise time (0.29 ± 0.01 ms versus 0.52 ± 0.04 ms, $P < 0.001$) and a higher action potential peak (84.8 ± 2.4 mV versus 65.6 ± 2.9 mV, $P < 0.001$). These data demonstrate that resident precursor cells in the BLA generate functional new neurons. Furthermore, the passive and active membrane properties of the GFP+ cells suggest that these newborn neurons are interneurons.

To confirm these findings, we conducted lineage tracing using $Ascl1^{CreERT2}$; $CAG^{floxStop\text{-}tdTomato}$ mice. As reported above, the majority of the resident population of precursor cells in the BLA express Ascl1 (Figure 1e and f). Therefore, whole-cell recordings were made from tdTom+ cells in the BLA at 4 and 8 weeks post-tamoxifen injection (Figure 5d-g and Supplementary Figure S5b). We found that tdTom+ neurons could fire trains of action potentials and receive excitatory inputs at both ages (4 weeks, $n = 5$ cells; 8 weeks, $n = 5$ cells; Figure 5f and g and Supplementary Figure S4d-f). Similar to GFP+ cells, tdTom+ cells had different active and passive membrane properties from those of principal neurons (Figure 5h and i and Supplementary Figure S4g–j) indicating that these newborn cells are interneurons. In particular, the action potentials of the tdTom+ cells at both 4 and 8 weeks were significantly faster than those of principal neurons with a half-width of 0.92 ± 0.05 ms ($n = 5$, $P < 0.01$) and 0.87 ± 0.05 ms ($n = 5$, $P < 0.001$), respectively (Figure 5i). To further support our electrophysiological findings and to immunohistochemically characterize these newborn cells in $Ascl1^{CreERT2}$; $CAG^{floxStop\text{-}tdTomato}$ mice at 4 weeks post tamoxifen treatment, we stained for calcium binding protein calbindin and calretinin, which are widely used as interneuron markers and label the majority (>70%) of interneurons in the BLA.[41,45] We found that ~85% (13 out of 15) of tdTom+ cells expressed calbindin (Supplementary Figure 5), with one cell expressing both calbindin and calretinin

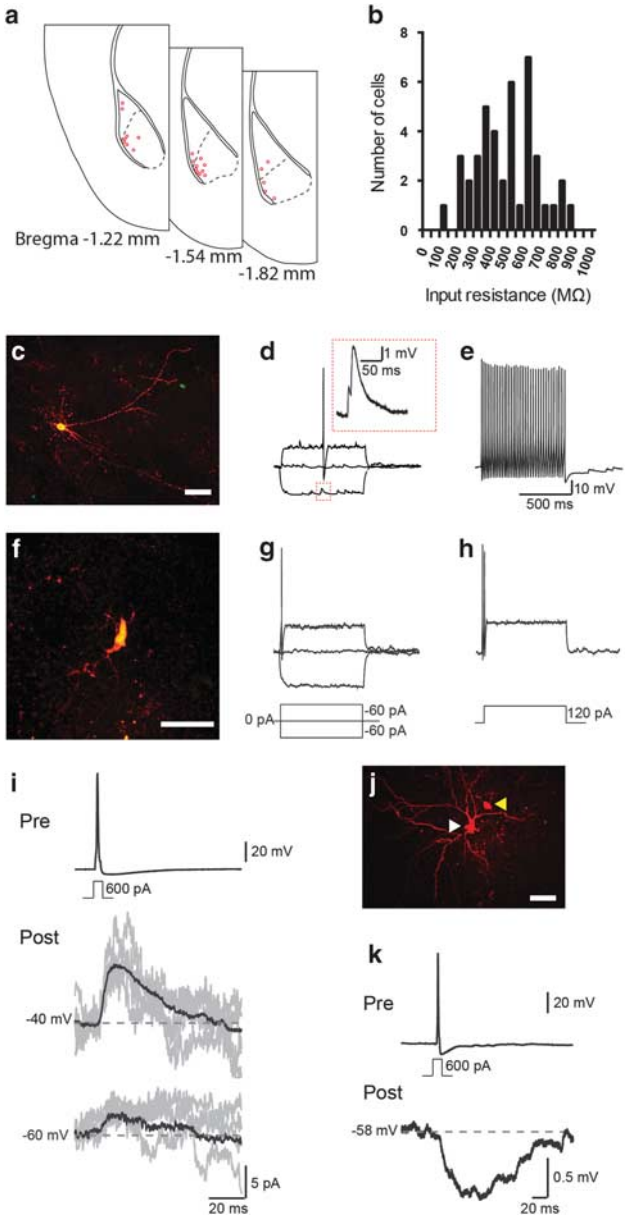

Figure 4. DCX-GFP-expressing cells in the basolateral amygdala (BLA) exhibit the electrophysiological properties of interneurons. (**a**) Location of recovered cells in the BLA ($n = 23$ cells). (**b**) Histogram showing the distribution of input resistance of DCX- GFP+ cells ($n = 42$ cells), measured using whole-cell recordings. Recovered cells displayed morphologies ranging from cells with branching dendrites (**c**), that had interneuron-like fast-spiking firing properties (**d**, **e**) and high spontaneous activity (d: inset), to sparsely branching, underdeveloped cells (**f**), which fired fewer action potentials (**g**, **h**). Firing was evoked using increasing steps of current injection (as shown below in **g** and **h**). (**i**) Dual whole-cell recording shows that a DCX-GFP+ cell is capable of forming inhibitory connections onto pyramidal cells (1 paired recording out of 6 dual recordings); an evoked action potential in the presynaptic cell ('Pre'; recovered cell indicated by white arrowhead in **j**) evoked an outward postsynaptic current in the postsynaptic cell ('Post'; recovered cell indicated by yellow arrowhead in **j**) when voltage-clamped at − 40 mV (9.50 ± 0.54 pA; 4.27 ± 0.62 pA at − 60 mV, close to the chloride reversal potential). Black traces show the average response with example traces of single episodes in gray. (**k**) In current clamp this response was an inhibitory postsynaptic potential in the postsynaptic cell (−0.78 ± 0.09 mV). Scale bars, 50 μm in (**c**), 25 μm in (**f**) and 50 μm in (**j**).

(Supplementary Figure 5d). Taken together, electrophysiological recordings and marker expression show that Ascl1-expressing precursor cells within the adult BLA generate new functional interneurons.

Notably, the input resistance of the tdTom+ cells at 4 weeks (343.0 ± 35.1 MΩ, $n = 5$) was significantly higher than that observed for these cells at 8 weeks (172.5 ± 32.4 MΩ, $n = 5$, $P = 0.001$) or the GFP+ cells at 8 weeks post-infection (173.4 ± 19.3 MΩ, $n = 6$, $P = 0.002$; Figure 5h). This decrease in input resistance over time is consistent with that observed during the maturation of newborn granule cells in the dentate gyrus,[39,46] suggesting that newborn neurons in the BLA display a similar progression from an immature to mature state.

Contextual fear conditioning has no effect on precursor cell numbers or proliferation in the amygdala

A growing body of data has demonstrated a strong causal link between adult neurogenesis and learning in the hippocampus.[9,47,48] As the amygdala and hippocampus have strong neural connections, and both play roles in contextual fear conditioning,[49] we tested the effects of this paradigm on cell proliferation in these two brain regions (Figure 6a). As expected, fear training resulted in significant freezing to the context in conditioned mice (54 ± 6% freezing), compared to the control mice that showed very little freezing (Figure 6b). Using the neurosphere assay to quantify precursor activity, we found no difference in the number of amygdala-derived neurospheres generated following fear conditioning (Figure 6e), and the average size of these neurospheres did not vary significantly between the naive control and conditioned groups (Figure 6f; diameter of neursopheres in control group: 78.5 ± 10.5 μm versus conditioned group: 60.9 ± 5.6 μm). Moreover, no significant correlation was found between the number or size of neurospheres obtained, or the level of freezing (data not shown). Similarly, fear conditioning did not significantly alter the number or size of the neurospheres generated from hippocampi harvested from the same animals (Figure 6c and d).

As there was no change in the number or proliferative potential of resident precursor cells in the amygdala following fear conditioning, we also examined the status of proliferating cells within the amygdala *in vivo*. Overall, a similar number of BrdU+ cells were observed in the control and conditioned groups (Figure 6c). Moreover, no significant relationship was found between the level of freezing, and the number of BrdU+ cells ($r = -0.37$, $P > 0.05$). Interestingly, however, a significant increase in the number of BrdU+ cells was observed in the dentate gyrus of conditioned mice compared to the control (Figure 6d). Together, these findings indicate that, although fear conditioning does not alter the activity of resident precursor cells or cell proliferation within the amygdala, it selectively enhances cell proliferation in the hippocampal dentate gyrus.

DISCUSSION

In this study, we provide evidence that the amygdala is a *bona fide* neurogenic region in the adult brain. We show that an endogenous population of precursor cells, a large proportion of which express the proneural gene Ascl1, is present in the adult BLA. *In vitro*, these precursor cells proliferate and differentiate to exhibit immunohistochemical and electrophysiological properties that are characteristic of neurons. Consistent with our findings *in vitro*, we also demonstrate the presence of proliferating cells in the BLA *in vivo*, a proportion of which differentiate into mature neurons and display the electrophysiological and immunohistochemical properties characteristic of interneurons.

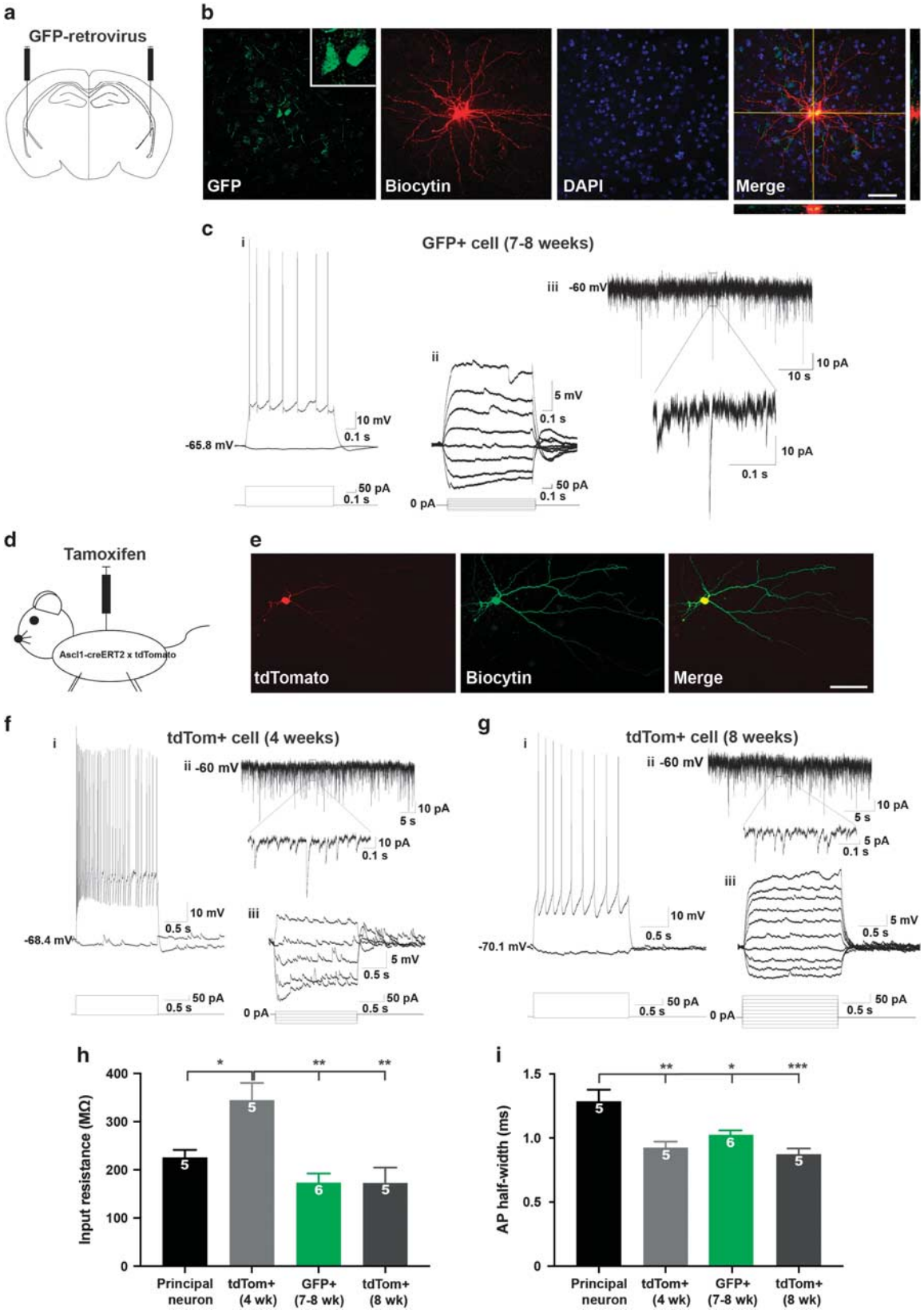
a
GFP-retrovirus
b
GFP
Biocytin
DAPI
Merge
c
GFP+ cell (7-8 weeks)
i
10 mV
0.1 s
-65.8 mV
50 pA
0.1 s
ii
5 mV
0.1 s
50 pA
0.1 s
0 pA
iii -60 mV
10 pA
10 s
10 pA
0.1 s
d
Tamoxifen
Ascl1-creERT2 x tdTomato
e
tdTomato
Biocytin
Merge
f
tdTom+ cell (4 weeks)
i
10 mV
0.5 s
-68.4 mV
50 pA
0.5 s
ii -60 mV
10 pA
5 s
10 pA
0.1 s
iii
5 mV
0.5 s
50 pA
0.5 s
0 pA
g
tdTom+ cell (8 weeks)
i
10 mV
0.5 s
-70.1 mV
50 pA
0.5 s
ii -60 mV
10 pA
5 s
5 pA
0.1 s
iii
5 mV
0.5 s
50 pA
0.5 s
0 pA
h
Input resistance (MΩ)
400
300
200
100
0
5
5
6
5
Principal neuron
tdTom+ (4 wk)
GFP+ (7-8 wk)
tdTom+ (8 wk)
i
AP half-width (ms)
1.5
1.0
0.5
0
5
5
6
5
Principal neuron
tdTom+ (4 wk)
GFP+ (7-8 wk)
tdTom+ (8 wk)

Our analysis of the precursor cells within the amygdala suggests that, although these cells do share some properties with those present in the SVZ and hippocampal niches, precursors in the BLA form a distinct population. First, using the neurosphere assay, we find that this population is much smaller than that present in the hippocampus[26] or the SVZ.[26,50] Second, unlike the hippocampus, but similar to the SVZ, the amygdala does not contain any populations of latent precursor cells that can be activated by depolarizing levels of KCl[4] or norepinephrine.[27] However, as both these treatments evoked a significant increase in the size of amygdala-derived neurospheres, it appears that these stimuli play a pro-proliferative role. This is in contrast to the effect of KCl on the SVZ-derived neural precursor cell population, where a significant reduction in precursor numbers has been noted.[4] Although the precise phenotypic identity of this small pool of precursor cells in the BLA remains to be determined, our data show that a large proportion of them express Ascl1, similar to results obtained in the other known neurogenic niches.[35]

Several lines of evidence demonstrate that precursor cells isolated from the BLA are neurogenic. First, differentiated neurospheres derived from this region of Thy1-YFP mice contained YFP+ cells. Second, these cells had the morphological features of neurons and expressed the neuronal marker βIII tubulin. Finally, whole-cell recordings from YFP-expressing cells showed that they

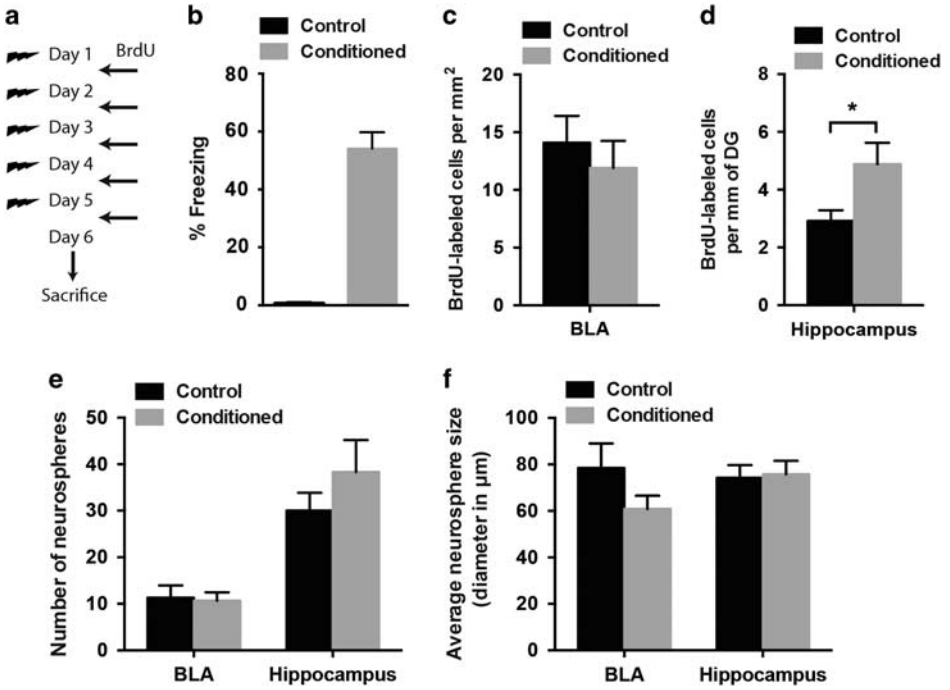

Figure 6. Fear learning has no effect on precursor cell activity and cell proliferation in the basolateral amygdala (BLA) (**a**) Schematic of the contextual fear conditioning protocol and BrdU administration. (**b**) All animals showed robust context fear conditioning ($n = 8$ in each group). (**c**, **d**) There was a significant increase in the number of BrdU-labeled cells in the dentate gyrus (DG) of the hippocampus (**f**) following fear conditioning, but no change in the number of BrdU-labeled cells in the BLA (**e**) of conditioned versus control animals (conditioned: $n = 6$, control: $n = 7$; $^{*}P < 0.05$). (**e**, **f**) There was no change in the number (**e**) or size (**f**) of neurospheres in the BLA or hippocampus following contextual fear conditioning (conditioned: $n = 13$, control: $n = 12$).

Figure 5. Functional properties of new neurons in the basolateral amygdala (BLA) using retrovirus labeling and lineage tracing. (**a**) A schematic illustrating bilateral injections of green fluorescent protein (GFP)-retrovirus in the BLA of 8-week-old C57BL/6 J mice. (**b**) Example GFP+ neurons (green) in the BLA recovered from whole-cell patch-clamp recordings and filled with biocytin (red). Note the presence of a doublet. Nuclei are stained with DAPI (blue). Scale bar, 50 μm (**c**) Whole-cell patch-clamp recordings from one GFP+ cell of the doublet showing (i) a train of action potentials induced by a +190 pA current injection, (ii) an example of spontaneous excitatory potential recording while injecting current steps from −60 to +80 pA, and (iii) an example trace of sEPSCs recorded while holding the cell at −60 mV. (**d**) Schematic showing tamoxifen injection in $Ascl1^{CreERT2}$; $CAG^{floxStop\text{-}tdTomato}$ mice. (**e**) An example of a tdTom+ cell (red) in the BLA, 4 weeks after the last tamoxifen injection, which was recovered with biocytin (green) following whole-cell patch-clamp recordings. Scale bar, 50 μm (**f**) An example of whole-cell patch-clamp recordings of a tdTom+ cell at 4 weeks post-tamoxifen showing (**i**) a train of action potentials induced by +190 pA current injection, (ii) an example trace of sEPSCs recorded while holding the cell at −60 mV, and (iii) an example of a spontaneous excitatory potential recording while injecting current steps from −60 to +20 pA. (**g**) An example of whole-cell patch-clamp recordings from a tdTom+ cell at 8 weeks post-tamoxifen showing (**i**) a train of action potentials induced by +240 pA current injection, (ii) an example trace of sEPSCs recorded while holding the cell at −60 mV, and (iii) an example of a spontaneous excitatory potential recording while injecting current steps from −60 to +120 pA. (**h**) Graph showing the input resistances of recorded cells in the BLA. Note that the tdTom+ cells at 4 weeks have higher input resistance than the input resistances of principal neurons ($n = 5$, $^{*}P < 0.05$), retrovirus-GFP+ cells at 7–8 weeks ($n = 6$, $^{**}P < 0.01$), and tdTom+ cells at 8 weeks ($n = 6$, $^{**}P < 0.01$). (**i**) Graph showing action potential half-widths from recorded cells within the BLA. Principal neurons have a half-width ($n = 5$) that is slower than the half-widths of tdTom+ cells at 4 weeks ($n = 5$, $^{**}P < 0.01$), GFP+ cells at 7–8 weeks ($n = 6$, $^{*}P < 0.05$), and tdTom+ cells at 8 weeks ($n = 5$, $^{***}P < 0.001$).

had a resting membrane potential, and could discharge small amplitude action potentials, demonstrating that amygdala precursor cells proliferate and differentiate into functional neurons *in vitro*. Consistent with the presence of neurogenic precursor cells in this nucleus, BrdU labeling revealed the presence of newly generated cells in the BLA.[22–24] Importantly, a proportion of these newly generated cells expressed DCX, the expression of which has been widely used as a surrogate marker of neurogenesis in the adult brain. Moreover, using DCX-GFP mice, we demonstrate that ~ 23% of the GFP+ cells in the BLA incorporated BrdU, indicating that they represent newly generated cells. These GFP+ cells had sparsely spiny dendrites, and electrophysiological recordings showed that they had relatively short duration action potentials, and discharged at high frequency, suggesting that they were interneurons.[41,51] These cells also displayed spontaneous excitatory synaptic potentials, demonstrating that they receive synaptic input, and paired recording showed that DCX-GFP+ cells can make inhibitory synaptic synapses onto local principal neurons.

Importantly, GFP-retrovirus injection in the BLA revealed the presence of newborn neurons 7–8 weeks after infection. Similar to DCX-GFP+ cells, these cells had short duration action potentials, passive and active membrane properties different from those of principal neurons, and received spontaneous excitatory synaptic potentials, supporting the idea that the precursor cells in the BLA mature into functional interneurons that integrate and connect to other cells. Using Ascl1^{CreERT2}; CAG$^{floxStop\text{-}tdTomato}$ mice, in which the lineage of newborn cells can be traced using tamoxifen, we showed that 4 and 8-week-old new neurons exhibited passive and active membrane properties similar to those seen in DCX-GFP, and retrovial-injected animals. Moreover, all three methods demonstrated that the newly born neurons display spontaneous excitatory synaptic potentials, indicating that these neurons are functional and integrate into the amygdala circuitry, similar to what is seen in the dentate gyrus.[39,46]

Previous reports have shown that no or very few BrdU-labeled cells in the amygdala of rodents co-express the mature neuronal marker NeuN,[23–25] suggesting that the adult amygdala is non-neurogenic. In one study that did report the neurogenic fate of BrdU-labeled proliferating cells in the amygdala,[52] a high proportion of these cells displayed a neuronal phenotype within 24 h of BrdU injection, making it difficult to interpret whether these were proliferating precursors or neurons undergoing DNA repair. In another study, cell proliferation was observed in the amygdala of PTZ-treated (epileptic) rats.[53] However, as no quantification was presented, the extent and proportion of proliferating cells that adopted a neuronal fate remained unknown. Our results show that new neurons are generated in the BLA, and express the neuronal markers DCX and NeuN. The failure to detect newly generated neurons in the amygdala in previous studies could be due to differences in the dosage or length of BrdU administration.

Our electrophysiological recordings suggest that the DCX-GFP+ cells, retrovirus-GFP+ cells and tdTom+ cells derived from Ascl1-expressing precursor cells in the BLA are interneurons. Furthermore, we find that majority of 4 week-old tdTom+ cells express interneuron marker calbindin. Given that newborn neurons in the hippocampal dentate gyrus are glutamatergic,[47] we suggest that the newborn cells in the BLA may in fact represent a distinct population that differs in its electrophysiological characteristics from that generated in the hippocampus. Furthermore, our results reveal that this distinct population of new neurons within the BLA survives for at least 8 weeks after their birth. This supports the idea that precursor cells within the BLA give rise to mature and functional interneurons, which are likely to play a role in shaping the physiology of this nucleus. It will be interesting to determine whether the numbers of neural precursors and new neurons in the amygdala decline with aging. In this regard, it is worth noting that a population of cells that co-express the polysialylated form of the neural cell adhesion molecule and DCX has also been reported in the amygdala of postmortem human brains.[54] Given a recent report that suggests the persistence of neurogenesis in the hippocampus of adult humans throughout life,[21,55] together with studies showing the presence of adult-born neurons in the amygdala of both Old World and New World monkeys,[21] and the persistence of DCX+ cells in aged non-human primates,[56] it is possible that the generation of new neurons may also persist in the amygdala of adult humans. Future studies using the elegant ^{14}C retrospective birth-dating technique may shed more light on this issue.

The functional significance of the neurogenic precursor cells in the amygdala of rodents remains unclear. We did not detect any effect of contextual fear conditioning on either precursor cell numbers or cell proliferation. In contrast, the application of norepinephrine or KCl clearly increased the size of neurospheres *in vitro*. The extent of norepinephrine release and/or the level of neuronal activity that is required to enhance precursor proliferation following contextual fear conditioning *in vivo* is currently not known, and may be influenced by the amplitude, duration or temporal delay in the pairing of the shock and the context. Moreover, it is possible that fear conditioning leads to alterations in other factors *in vivo* that negatively influence cell proliferation and abrogate any proliferation-enhancing effects of norepinephrine or neuronal activity. Nonetheless, the link between contextual fear learning, which involves the activity of the amygdala and the hippocampus, is interesting, given our findings of an increase in the number of BrdU-labeled cells in the hippocampus but not the amygdala of fear-conditioned mice. A recent study has shown a significant reduction in hippocampal cell proliferation following either lesion- or viral-mediated attenuation of BLA activity in mice.[57] Interestingly, BLA lesions also significantly decreased the expression of the activity-regulated gene c-Fos in DCX+ newborn cells in the hippocampus. As BLA activity is known to support long-term potentiation in the dentate gyrus,[58] it seems likely that the enhancement in proliferation observed in the granule cell layer of the hippocampus in this study is congruent with the increase in BLA activity during fear learning. Whether the increase in proliferation in the dentate gyrus following fear conditioning is a direct consequence of enhanced long-term potentiation[28,59] or mediated via the release of neurotransmitters such as glutamate, norepinephrine or acetylcholine[27,60,61] remains unknown. It should be noted that, as our control mice were not exposed to the context, we can not exclude the possibility that the increase in the number of BrdU+ cells seen in the hippocampus in the conditioned group compared to the control is partly due to the novel context rather than contextual fear learning.

In summary, we have demonstrated the presence of neural precursors and the generation of new interneurons in the BLA of adult mice. Although we did not observe learning-induced changes in precursor proliferation in this nucleus, the possibility that new neurons in this region of the amygdala contribute towards fear-related memory remains to be investigated.

CONFLICT OF INTEREST

The authors declare no conflict of interest.

ACKNOWLEDGMENTS

This work was supported by grants from the National Health and Medical Research Council of Australia to PFB and PS (NHMRC Program Grants: 301204 and 569575; Project Grant:10768227) and by Mater Foundation Fellowship to DJJ. We thank Hongjun Song (Johns Hopkins Medical School) for the retroviral vectors, Imogen

O'Keeffe, Li Xu and Wendy Lee for technical assistance and Rowan Tweedale and Ashley Cooper for editorial assistance.

REFERENCES

1 Ming GL, Song H. Adult neurogenesis in the mammalian central nervous system. *Annu Rev Neurosci* 2005; **28**: 223–250.
2 Imayoshi I, Sakamoto M, Ohtsuka T, Takao K, Miyakawa T, Yamaguchi M *et al.* Roles of continuous neurogenesis in the structural and functional integrity of the adult forebrain. *Nat Neurosci* 2008; **11**: 1153–1161.
3 Rietze RL, Valcanis H, Brooker GF, Thomas T, Voss AK, Bartlett PF. Purification of a pluripotent neural stem cell from the adult mouse brain. *Nature* 2001; **412**: 736–739.
4 Walker TL, White A, Black DM, Wallace RH, Sah P, Bartlett PF. Latent stem and progenitor cells in the hippocampus are activated by neural excitation. *J Neurosci* 2008; **28**: 5240–5247.
5 Arruda-Carvalho M, Sakaguchi M, Akers KG, Josselyn SA, Frankland PW. Posttraining ablation of adult-generated neurons degrades previously acquired memories. *J Neurosci* 2011; **31**: 15113–15127.
6 Enwere E, Shingo T, Gregg C, Fujikawa H, Ohta S, Weiss S. Aging results in reduced epidermal growth factor receptor signaling, diminished olfactory neurogenesis, and deficits in fine olfactory discrimination. *J Neurosci* 2004; **24**: 8354–8365.
7 Shors TJ, Miesegaes G, Beylin A, Zhao M, Rydel T, Gould E. Neurogenesis in the adult is involved in the formation of trace memories. *Nature* 2001; **410**: 372–376.
8 Snyder JS, Hong NS, McDonald RJ, Wojtowicz JM. A role for adult neurogenesis in spatial long-term memory. *Neuroscience* 2005; **130**: 843–852.
9 Vukovic J, Borlikova GG, Ruitenberg MJ, Robinson GJ, Sullivan RK, Walker TL *et al.* Immature doublecortin-positive hippocampal neurons are important for learning but not for remembering. *J Neurosci* 2013; **33**: 6603–6613.
10 Santarelli L, Saxe M, Gross C, Surget A, Battaglia F, Dulawa S *et al.* Requirement of hippocampal neurogenesis for the behavioral effects of antidepressants. *Science* 2003; **301**: 805–809.
11 Gould E, Beylin A, Tanapat P, Reeves A, Shors TJ. Learning enhances adult neurogenesis in the hippocampal formation. *Nat Neurosci* 1999; **2**: 260–265.
12 Kokoeva MV, Yin H, Flier JS. Neurogenesis in the hypothalamus of adult mice: potential role in energy balance. *Science* 2005; **310**: 679–683.
13 Zhao M, Momma S, Delfani K, Carlen M, Cassidy RM, Johansson CB *et al.* Evidence for neurogenesis in the adult mammalian substantia nigra. *Proc Natl Acad Sci USA* 2003; **100**: 7925–7930.
14 Gould E. How widespread is adult neurogenesis in mammals? *Nat Rev Neurosci* 2007; **8**: 481–488.
15 Nowakowski RS, Hayes NL. New neurons: extraordinary evidence or extraordinary conclusion? *Science* 2000; **288**: 771.
16 Rakic P. Neurogenesis in adult primate neocortex: an evaluation of the evidence. *Nat Rev Neurosci* 2002; **3**: 65–71.
17 Davis M, Whalen PJ. The amygdala: vigilance and emotion. *Mol Psychiatry* 2001; **6**: 13–34.
18 LeDoux JE. Emotion circuits in the brain. *Ann Rev Neurosci* 2000; **23**: 155–184.
19 Likhtik E, Paz R. Amygdala-prefrontal interactions in (mal)adaptive learning. *Trends Neurosci* 2015; **38**: 158–166.
20 Miller BR, Hen R. The current state of the neurogenic theory of depression and anxiety. *Curr Opin Neurobiol* 2015; **30C**: 51–58.
21 Bernier PJ, Bedard A, Vinet J, Levesque M, Parent A. Newly generated neurons in the amygdala and adjoining cortex of adult primates. *Proc Natl Acad Sci USA* 2002; **99**: 11464–11469.
22 Goncalves L, Silva R, Pinto-Ribeiro F, Pego JM, Bessa JM, Pertovaara A *et al.* Neuropathic pain is associated with depressive behaviour and induces neuroplasticity in the amygdala of the rat. *Exp Neurol* 2008; **213**: 48–56.
23 Okuda H, Tatsumi K, Makinodan M, Yamauchi T, Kishimoto T, Wanaka A. Environmental enrichment stimulates progenitor cell proliferation in the amygdala. *J Neurosci Res* 2009; **87**: 3546–3553.
24 Wennstrom M, Hellsten J, Tingstrom A. Electroconvulsive seizures induce proliferation of NG2-expressing glial cells in adult rat amygdala. *Biol Psychiatry* 2004; **55**: 464–471.
25 Ehninger D, Wang LP, Klempin F, Romer B, Kettenmann H, Kempermann G. Enriched environment and physical activity reduce microglia and influence the fate of NG2 cells in the amygdala of adult mice. *Cell Tissue Res* 2011; **345**: 69–86.
26 Bull ND, Bartlett PF. The adult mouse hippocampal progenitor is neurogenic but not a stem cell. *J Neurosci* 2005; **25**: 10815–10821.
27 Jhaveri DJ, Mackay EW, Hamlin AS, Marathe SV, Nandam LS, Vaidya VA *et al.* Norepinephrine directly activates adult hippocampal precursors via beta3-adrenergic receptors. *J Neurosci* 2010; **30**: 2795–2806.
28 Kameda M, Taylor CJ, Walker TL, Black DM, Abraham WC, Bartlett PF. Activation of latent precursors in the hippocampus is dependent on long-term potentiation. *Transl Psychiatry* 2012; **2**: e72.
29 Sah P, Faber ES, Lopez De Armentia M, Power J. The amygdaloid complex: anatomy and physiology. *Physiol Rev* 2003; **83**: 803–834.
30 Pape HC, Pare D. Plastic synaptic networks of the amygdala for the acquisition, expression, and extinction of conditioned fear. *Physiol Reviews* 2010; **90**: 419–463.
31 Feng G, Mellor RH, Bernstein M, Keller-Peck C, Nguyen QT, Wallace M *et al.* Imaging neuronal subsets in transgenic mice expressing multiple spectral variants of GFP. *Neuron* 2000; **28**: 41–51.
32 Spampanato J, Sullivan RK, Turpin FR, Bartlett PF, Sah P. Properties of doublecortin expressing neurons in the adult mouse dentate gyrus. *PLoS ONE* 2012; **7**: e41029.
33 Okabe M, Ikawa M, Kominami K, Nakanishi T, Nishimune Y. 'Green mice' as a source of ubiquitous green cells. *FEBS Lett* 1997; **407**: 313–319.
34 Tamamaki N, Yanagawa Y, Tomioka R, Miyazaki J, Obata K, Kaneko T. Green fluorescent protein expression and colocalization with calretinin, parvalbumin, and somatostatin in the GAD67-GFP knock-in mouse. *J Comp Neurol* 2003; **467**: 60–79.
35 Kim EJ, Ables JL, Dickel LK, Eisch AJ, Johnson JE. Ascl1 (Mash1) defines cells with long-term neurogenic potential in subgranular and subventricular zones in adult mouse brain. *PLoS ONE* 2011; **6**: e18472.
36 Tashiro A, Makino H, Gage FH. Experience-specific functional modification of the dentate gyrus through adult neurogenesis: a critical period during an immature stage. *J Neurosci* 2007; **27**: 3252–3259.
37 Reynolds BA, Rietze RL. Neural stem cells and neurospheres--re-evaluating the relationship. *Nat Methods* 2005; **2**: 333–336.
38 Andersen J, Urban N, Achimastou A, Ito A, Simic M, Ullom K *et al.* A transcriptional mechanism integrating inputs from extracellular signals to activate hippocampal stem cells. *Neuron* 2014; **83**: 1085–1097.
39 Yang SM, Alvarez DD, Schinder AF. Reliable genetic labeling of adult-born dentate granule cells using Ascl1 CreERT2 and Glast CreERT2 murine lines. *J Neurosci* 2015; **35**: 15379–15390.
40 Mahanty NK, Sah P. Calcium-permeable AMPA receptors mediate long-term potentiation in interneurons in the amygdala. *Nature* 1998; **394**: 683–687.
41 Spampanato J, Polepalli J, Sah P. Interneurons in the basolateral amygdala. *Neuropharmacology* 2011; **60**: 765–773.
42 Ma DK, Jang MH, Guo JU, Kitabatake Y, Chang ML, Pow-Anpongkul N *et al.* Neuronal activity-induced Gadd45b promotes epigenetic DNA demethylation and adult neurogenesis. *Science* 2009; **323**: 1074–1077.
43 van Praag H, Schinder AF, Christie BR, Toni N, Palmer TD, Gage FH. Functional neurogenesis in the adult hippocampus. *Nature* 2002; **415**: 1030–1034.
44 Zhao C, Teng EM, Summers RG Jr, Ming GL, Gage FH. Distinct morphological stages of dentate granule neuron maturation in the adult mouse hippocampus. *J Neurosci* 2006; **26**: 3–11.
45 Kemppainen S, Pitkanen A. Distribution of parvalbumin, calretinin, and calbindin-D(28k) immunoreactivity in the rat amygdaloid complex and colocalization with gamma-aminobutyric acid. *J Comp Neurol* 2000; **426**: 441–467.
46 Gu Y, Arruda-Carvalho M, Wang J, Janoschka SR, Josselyn SA, Frankland PW *et al.* Optical controlling reveals time-dependent roles for adult-born dentate granule cells. *Nat Neurosci* 2012; **15**: 1700–1706.
47 Deng W, Aimone JB, Gage FH. New neurons and new memories: how does adult hippocampal neurogenesis affect learning and memory? *Nat Rev Neurosci* 2010; **11**: 339–350.
48 Saxe MD, Malleret G, Vronskaya S, Mendez I, Garcia AD, Sofroniew MV *et al.* Paradoxical influence of hippocampal neurogenesis on working memory. *Proc Natl Acad Sci USA* 2007; **104**: 4642–4646.
49 Maren S. Neurobiology of Pavlovian fear conditioning. *Annu Rev Neurosci* 2001; **24**: 897–931.
50 Blackmore DG, Golmohammadi MG, Large B, Waters MJ, Rietze RL. Exercise increases neural stem cell number in a growth hormone-dependent manner, augmenting the regenerative response in aged mice. *Stem Cells* 2009; **27**: 2044–2052.
51 McDonald AJ. Calbindin-D28k immunoreactivity in the rat amygdala. *J Comp Neurol* 1997; **383**: 231–244.
52 Fowler CD, Freeman ME, Wang Z. Newly proliferated cells in the adult male amygdala are affected by gonadal steroid hormones. *J Neurobiol* 2003; **57**: 257–269.
53 Park JH, Cho H, Kim H, Kim K. Repeated brief epileptic seizures by pentylenetetrazole cause neurodegeneration and promote neurogenesis in discrete brain regions of freely moving adult rats. *Neuroscience* 2006; **140**: 673–684.
54 Marti-Mengual U, Varea E, Crespo C, Blasco-Ibanez JM, Nacher J. Cells expressing markers of immature neurons in the amygdala of adult humans. *Eur J Neurosci* 2013; **37**: 10–22.

55 Spalding KL, Bergmann O, Alkass K, Bernard S, Salehpour M, Huttner HB *et al.* Dynamics of hippocampal neurogenesis in adult humans. *Cell* 2013; **153**: 1219–1227.
56 Zhang XM, Cai Y, Chu Y, Chen EY, Feng JC, Luo XG *et al.* Doublecortin-expressing cells persist in the associative cerebral cortex and amygdala in aged nonhuman primates. *Front Neuroanat* 2009; **3**: 17.
57 Kirby ED, Friedman AR, Covarrubias D, Ying C, Sun WG, Goosens KA *et al.* Basolateral amygdala regulation of adult hippocampal neurogenesis and fear-related activation of newborn neurons. *Mol Psychiatry* 2012; **17**: 527–536.
58 Ikegaya Y, Saito H, Abe K. The basomedial and basolateral amygdaloid nuclei contribute to the induction of long-term potentiation in the dentate gyrus in vivo. *Eur J Neurosci* 1996; **8**: 1833–1839.
59 Bruel-Jungerman E, Davis S, Rampon C, Laroche S. Long-term potentiation enhances neurogenesis in the adult dentate gyrus. *J Neurosci* 2006; **26**: 5888–5893.
60 Itou Y, Nochi R, Kuribayashi H, Saito Y, Hisatsune T. Cholinergic activation of hippocampal neural stem cells in aged dentate gyrus. *Hippocampus* 2011; **21**: 446–459.
61 Joo JY, Kim BW, Lee JS, Park JY, Kim S, Yun YJ *et al.* Activation of NMDA receptors increases proliferation and differentiation of hippocampal neural progenitor cells. *J Cell Sci* 2007; **120**(Pt 8): 1358–1370.

Supplementary Information accompanies the paper on the *Molecular Psychiatry* website (http://www.nature.com/mp)